(3NF) was introduced. The first applications of such a force showed that it brings a sizable contribution to observables and cannot be ignored [11]. The contribution of the 3NF can be examined e.g. by comparing binding energies of light nuclei calculated with and without this part of the Hamiltonian ~~concerning~~ experimental values.

For example, the binding energy[1] for ^{3}H calculated with the Argonne V18 (AV18) 2N potential without 3NF amounts to $E_b(^3\mathrm{H}) = -7.628\,\mathrm{MeV}$ [12]. There are different models that might add a 3NF contribution to AV18 (or other potentials). Using the Tucson-Melbourne (TM) model [13] results in $E_b(^3\mathrm{H}) = -8.478\,\mathrm{MeV}$, and the Urbana IX [14] 3NF provides us with $E_b(^3\mathrm{H}) = -8.484\,\mathrm{MeV}$. Looking at the experimental value $E_b(^3\mathrm{H}) = -8.482\,\mathrm{MeV}$, it is clear that the 3NF contribution makes the prediction much closer to the measurement. Nevertheless, the parameters of the UrbanaIX 3NF were fitted to the experimental value for ^{3}H, so there is no surprise in good agreement.

However one can also check the binding energy for other nuclei, which were not used for the fitting. The 2N force (2NF) binding energy for ^{3}He (calculated with AV18) is $E_b(^3\mathrm{He}) = -6.917\,\mathrm{MeV}$. The TM contribution makes it $E_b(^3\mathrm{He}) = -7.706\,\mathrm{MeV}$, the Urbana IX gives $E_b(^3\mathrm{He}) = -7.739\,\mathrm{MeV}$, while the experimental value is $E_b(^3\mathrm{He}) = -7.718\,\mathrm{MeV}$. One can see the importance of 3NF contribution also for the α-particle's (^{4}He) binding energy: the AV18 alone gives $E_b(^4\mathrm{He}) = -24.25\,\mathrm{MeV}$, while the AV18 − TM leads to $-28.84\,\mathrm{MeV}$, the AV18 − Urbana IX delivers $E_b(^4\mathrm{He}) = -28.50\,\mathrm{MeV}$, and the experimental value is $-28.30\,\mathrm{MeV}$ [12].

Whereas the first applications included only early simplified "realistic" 3N potential, the latter investigations, based on more advanced models, fully confirmed ~~this~~ statements [15, 16]. Within new models, the four-nucleon (4N) interaction was constructed to improve the description of ^{4}He [17]. A broader discussion of nuclear forces used in this thesis is given below.

The electromagnetic force appears between charged particles like protons, electrons, or pions. That force acts also between charged particles and photons, so in photon- and electron- scatterings on the nuclei it is a necessary component of a description. However, electromagnetic interaction between nuclei manifests ~~only~~ at very low energies or for specific kinematic configurations with two protons having approximately equal momenta. Thus it ~~rather~~ is skipped in the lowest-order analysis.

The main contribution of electromagnetic interaction to disintegration processes in hand is due to the current operator describing photon-nucleon vertex and second-order processes. The structure of the electromagnetic current has been investigated in many works by numerous groups [18] but it was H. Arenhövel who performed a study of nuclear electromagnetic current in the few-nucleon sector. His long-term research, reviewed in [19] demonstrated various theoretical models applied to the deuteron photodisintegration. He analyzed among others a nonrelativistic potential model, a relativistic impulse approximation, and a relativistic meson-exchange model. These models were used to calculate the differential cross section and various polarization observables, which describe the probability of the process occurring at different scattering angles, photon energies, spin directions, etc.

The calculated cross sections were then compared to experimental data, and it was found that the relativistic meson-exchange model provided the best agreement with the data at photon's energies up to $E_\gamma \approx 100\,\mathrm{MeV}$. At higher energies agreement is observed but is getting worse. This model includes the exchange of virtual mesons between the interacting particles, which accounts for the strong and electromagnetic forces between

[1] More precisely it is a ground state energy, but I follow commonly used mental shortcut.

them.

Overall, Arenhövel demonstrated the importance of including both strong interaction and electromagnetic current operator in a description of the deuteron photodisintegration process, and highlighted the need for accurate theoretical models to interpret experimental data.

The weak force is of great importance in the study of nuclear processes. One of the main roles of the weak force is to mediate negative beta decay, which is a process in which a neutron in a nucleus is converted into a proton, emitting an electron and an antineutrino. This process plays a crucial role in the formation of elements in the universe, as it allows for the conversion of neutron-rich isotopes into more stable, proton-rich isotopes. Additionally, the weak force plays a role in neutrino interactions with matter, which are of great interest in both astrophysics and particle physics. In nuclear physics, weak interactions can also play a role in the decay of unstable nuclei, the production of neutrinos in nuclear reactions, and the scattering of neutrinos off nuclei. The study of weak interactions is therefore an essential component of the overall understanding of nuclear physics and the behavior of matter on the subatomic scale. However, in the thesis, I stick with electromagnetic processes.

Models of strong interaction used in the thesis

In order to model the nuclear potential, physicists often use phenomenological or semi-phenomenological approaches. It allows them to combine theoretical knowledge about the studied processes and experimental findings.

Among many of such models, the AV18 [19] force is one of the most advanced and therefore is used in the current thesis. To construct the nucleon-nucleon (NN) force, authors combine long-range one-pion-exchange part with short-range phenomenological one and supplement them with electromagnetic corrections. Free parameters were fitted to the Nijmegen partial-wave analysis of pp and np data [20]. Authors showed, that the AV18 potential delivers good description of nucleon-nucleon scattering data ($\chi^2/data = 1.08$ for around 4000 pp and np scattering data points) as well as deuteron properties (estimated binding energy is 2.2247(35) MeV vs experimental 2.224 575(9) MeV [21]).

Weinberg's idea of using chiral symmetry to describe nuclear interactions at low energies was first introduced in his papers published in 1990 and 1991 [22,23]. In these papers, Weinberg argued that the low-energy dynamics of nucleons could be described using a chiral Lagrangian, which is the most general Lagrangian consistent with chiral symmetry and its spontaneous breaking. This Lagrangian is expressed in terms of nucleon and pion fields, which are the degrees of freedom that become relevant at low energies.

The chiral Lagrangian is the starting point for the development of the Chiral Effective Field Theory (χEFT), which has become one of the most advanced approaches to low-energy nuclear physics [24]. The use of the χEFT allows (at least in theory) for the calculation of nuclear properties and reactions in a model-independent way. It is also possible to quantify the uncertainties associated with the calculation. One of the key features of the χEFT is that it allows for the construction of a nuclear potential, which can then be used in relevant formalisms, e.g. to solve the Schrödinger equation and to obtain bound and scattering state properties. The accuracy of the potential can be systematically improved by including higher-order terms in the chiral expansion, which leads to a better description of experimental data.

In the χEFT there are two natural scales: so-called soft scale $Q \sim M_\pi$ - the mass of

pion and the hard scale - $\Lambda_\chi \sim 0.7\,\text{GeV}$ - the chiral symmetry breaking scale. The ratio between these two scales Q/Λ_χ is being used as an expansion parameter in χEFT with power ν: $(Q/\Lambda_\chi)^\nu$. [2]

The possibility of deriving nuclear potential is an important feature of χEFT. The potential, as occurs in Lagrangian, is a perturbation expression of the same parameter Q/Λ_χ. Considering so-called irreducible diagrams (which cannot be split by cutting nucleon lines), Weinberg [22,23] came to the expression for the powers ν_W of such diagrams

$$\nu_W = 4 - A - 2C + 2L + \sum_i \Delta_i, \tag{1.1}$$

where i specifies a vertex number and

$$\Delta_i \equiv d_i + \frac{n_i}{2} - 2. \tag{1.2}$$

In Eq. (1.1) C is a number of pieces which are connected, L - the number of loops in the graph and A is the amount of nucleons in the diagram. In Eq. (1.2) n_i is a number of nucleon field operators and d_i - the number of insertions (or derivatives) of M_π.

Further analysis of Eq. (1.1) revealed some problems which occur for particular values of parameters in the equation, namely negative values of ν_W are possible while the order has to take integer values from 0 to infinity. To deal with that, Eq. (1.1) was slightly modified by adding $3A - 6$ to it [10,27]:

$$\nu = \nu_W + 3A - 6 = -2 + 2A - 2C + 2L + \sum_i \Delta_i. \tag{1.3}$$

That convention above is widely used and we will also stick to it as well.

In χEFT the first order, "leading order" ($\nu = 0$) is followed by the next-to-leading order ($\nu = 2$) [3], the next-to-next-to-leading order ($\nu = 3$) and so on. At each chiral order, new interaction diagrams complete the potential. There are only two diagrams at leading order (LO): one is a contact term and the other one is a one-pion exchange, see Fig. 1.1. Both diagrams reflect only 2NF. The same is for diagrams at next-to-leading order (NLO), where more contact terms occur together with two-pion exchange topologies. Each subsequent order includes more and more sophisticated diagrams describing nucleon interaction via multiple pion exchanges and various contact vertexes. 3NF appears for the first time at next-to-next-to-leading order (N^2LO) while 4NF contributions start from next-to-next-to-next-to-leading order (N^3LO). This scheme establishes for the first time a systematic way to include all the contributions to a strong nuclear force starting from the simplest diagrams at LO and gradually adding more and more terms. It is also beneficial in the way that one can obtain results using chiral potential at different orders and track which one gives a large or small contribution to the final prediction. At the moment, next-to-next-to-next-to-next-to-leading order (N^4LO) is the highest order at which 2N interaction has been completely derived. Nevertheless leading F-wave contact interactions from N^5LO have been combined with N^4LO force leading to the N^4LO^+ potential, which is currently regarded as the best available potential on the market. The progression of the chiral orders is reflected in a $\chi^2/data$. Leading order results in $\chi^2/data = 73$

[2] Note that exact values of some parameters are still under discussion [25]. We follow here approach proposed by E.Epelbaum and collaborators, see e.g. [26]

[3] The contributions to the potential at order $\nu = 1$ completely vanish due to parity and time-reversal invariance, so the next-to-leading order stands for the second order ($\nu = 2$) of expansion.

(with neutron-proton data with $E_{lab} = 0 - 100$MeV). Each subsequent order has better and better results: NLO gives $\chi^2/data = 2.2$, N^{2}LO - $\chi^2/data = 1.2$ and the highest, N^{4}LO$^+$, leads to $\chi^2/data = 1.08$ [26]. Similar progress is observed for a wider energy range, e.g for $E_{lab} = 0 - 300$MeV $\chi^2/data$ is 75, 14, 4.1, 2.01, 1.16 and 1.06 at LO, NLO, N^{2}LO, N^{3}LO, N^{4}LO and N^{4}LO$^+$, respectively. The proton-proton data description has a similar trend, so $\chi^2/data$ is 1380, 91, 41, 3.43, 1.67, 1.00 for the same energy bin and chiral orders. At N^{4}LO$^+$ $\chi^2/data$ for proton-proton data stands a similar value (close to 1) as for neutron-proton. However for the proton-proton force, the convergence comes a bit later, and the leading order has a way worse description than for the neutron-proton potential. In my work, I will use chiral potentials from LO up to N^{4}LO$^+$.

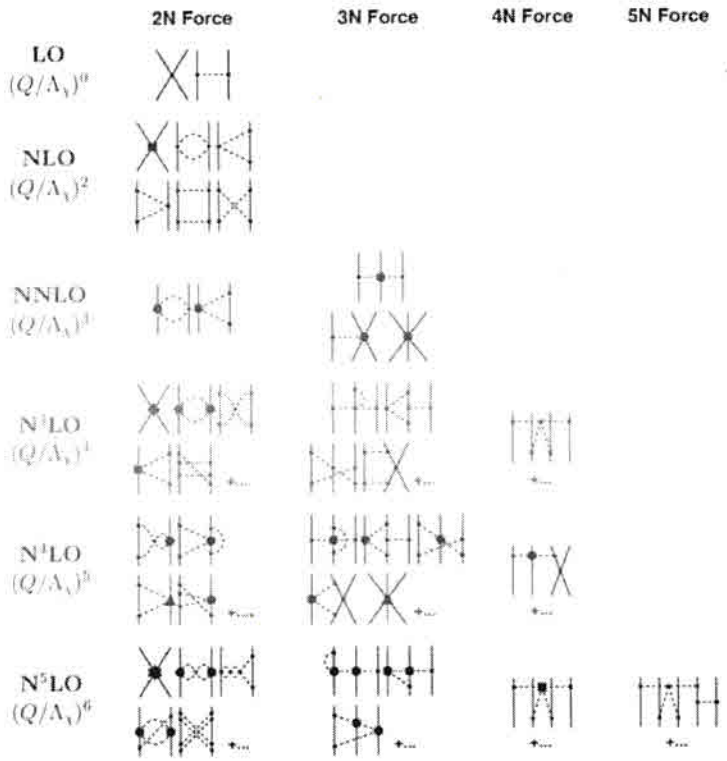

Figure 1.1: *Make own diagrams, e.g. with JaxoDraw or PyFeyn [28]*

The Argonne V18 potential [16], mentioned earlier, has 40 adjustable parameters, while χEFT NN potential at N^{4}LO [10] has only 27 low-energy constants (LECs) fitted to 2N data. The reduction of the number of free parameters of the χEFT-based potentials has not only a theoretical but also a practical advantage in the studies of nuclear systems.

The general scheme outlined above was developed mainly by the Bochum-Bonn and Moscow-Idaho groups. Both groups have similar approaches and were independently and almost simultaneously developing their models. In 1998 Epelbaum and collaborators from the Bochum-Bonn group presented a first version of their NN chiral potential [29, 30]. Developing more and more sophisticated versions with higher chiral orders, authors presented in 2001 [31] N^{2}LO model which included 3NF contributions and in 2005 [32] N^{3}LO NN potential. They were further developing their chiral model, taking into account more Feynmann diagrams coming to a higher chiral orders. At some moment Bochum-Bonn group faced a problem of potential regularisation [33, 34]. Solving it was a necessary step but authors were struggling with finding an appropriate regularization method to handle

the divergences that arise in the χEFT calculations. Different techniques were applied such as the cutoff regularization and the regulator function methods. An important step was done when authors started using a semi-local regularisation in the coordinate space. The corresponding potential is called the SCS potential (semi-local regularisation in the coordinate space) [35]. Later similar regularisation, but done in momentum space was introduced, resulting in the most advanced chiral potential [26]: the SMS. It is developed up to N^4LO^+ at the moment.

On the other side of the planet, in Idaho, R. Machleidt and his group from Moscow(Idaho) were also developing a chiral interaction. Their results from 2003 [36], following with later investigations [37, 38] and recently in [28] introduced very similar model to the one from the Bochum-Bonn group with minor technical differences.

There are a number of other attempts to construct the nuclear potential from the χEFT. M.Piarulli et al [39, 40] contributed to quite a similar approach, based on the same chiral potentials but including explicitly Δ-isobar intermediate states up to the third chiral order and taking into account sophisticated electromagnetic corrections.

Other groups try to improve already derived forces. Let us mention here works by A. Ekström and collaborators [11, 12] who, by using advanced fitting methods combined with statistical analysis proposed so-called optimised interaction V_{opt} which was proved to provide a good description of nuclei properties and nuclear matter without using 3NF.

Another approach is the pionless effective field theory, which integrates pions out and focuses on the various types of contact interactions between nucleons [13]. Obtained potential has a very simple form, but cannot be applied to higher energies since pions start playing an important role there.

Yet another promising approach is the Lattice Effective Field Theory (LEFT), which is based on the Lattice QCD simulations of the strong interaction. U.-G. Meißner and collaborators have developed a chiral effective theory for nuclear forces based on the methods of lattice QCD calculations [14]. This approach has the advantage of being able to predict the nuclear force directly from the first principles, without the need for phenomenological input. However, currently, it is limited to small systems and low energies due to the computational resources required for calculations. Up to now, the relatively simple two-nucleon scattering problem and few-nucleon bound state have been solved within the LEFT and more complex systems are still under attack. For more details please refer to [14].

Technically, the chiral potential may be derived both in coordinate and momentum spaces. Nevertheless, in both cases, it requires regularisation which improves potential behavior at small distances or at high momenta, which allows to avoid infinities. The SMS potential is being regularized semilocally. It means that local or nonlocal regularisations are being applied for different parts of the potential. In [32, 36] the non-local regulation scheme was applied to both short- and long-range parts of the potential while in the next model [28, 35] it affected only a short-range part. This regularisation is applied directly to the potential matrix elements in the coordinate space:

$$V_\pi(\vec{r}) \to V_{\pi,R}(\vec{r}) = V_\pi(\vec{r}) \left(1 - \exp\left(-r^2/R^2\right)\right), \tag{1.4}$$

or in the momentum space

$$V_\pi(\vec{p}', \vec{p}) \to V_\Lambda(\vec{p}', \vec{p}) = V_\pi(\vec{p}', \vec{p}) \exp\left[-(p'/\Lambda)^{2n} - (p/\Lambda)^{2n}\right], \tag{1.5}$$

where the cutoff R was chosen in the range of R = 0.8, ..., 1.2 fm, $\Lambda = \frac{2}{R}$ and n being

adjusted with respect to the considered chiral order. For specific case of the SMS force $\Lambda = 400 - 550\,\mathrm{MeV}$ and $n = 3$.

The other way of regularisation, the local one, is applied to the propagator operator, already during the derivation of potential. Namely, the Gaussian form factor $F(\vec{l}^2)$ is being used to reduce pions with higher momenta:

$$\int_{-\infty}^{\infty} \frac{\rho(\mu^2)}{\vec{l}^2 + \mu^2} d\mu^2 \to \frac{F(\vec{l}^2)}{\vec{l}^2 + \mu^2} \tag{1.6}$$

with

$$F(\vec{l}^2) = e^{-\frac{\vec{l}^2 + M_\pi^2}{\Lambda^2}}, \tag{1.7}$$

M_π is an effective pion mass, Λ - a cutoff parameter and l is a four-momentum of the exchanged pion. The form factor (1.7), being used together with Feynman propagator, ensures that the long-range part of the forces has no singularities.

The cut-off parameter Λ is not fixed and usually calculations are being performed for its different values. The comparison of such results may reveal stronger or weaker dependence on Λ and in a perfect case, which is expected at $\nu >> 1$, one will come up with such a potential, where the cut will not affect results at all. One of the aims of my thesis is to test how a big cut-off dependency of predictions is observed for the best currently available forces (SCS and SMS). To illustrate a cutoff dependency of the potential, in Fig. 1.2 I show values of the matrix elements for 2N $\langle p|V|p'\rangle$ potential ${}^3S_1 - {}^3D_1$ as a function of the momentum $|\vec{p}|$ with fixed value $|\vec{p}'|$=1.798 fm^{-1}. Please note, that the relatively strong dependency of specific matrix elements on the potential is not always leading to a strong dependency of observables, as observables comprise contributions from many matrix elements.

Let me add, that another regularisation function used by R. Machleidt and collaborators with non-local regulator only [28, 30]. That is the main reason for the observed differences between predictions based on Epelbaum's and Machleidt's models.

Currents

The electromagnetic current operator for a few-nucleon system has both one- and many-body contributions, which can be denoted as j^1_μ, j^2_μ, j^3_μ, etc, respectively (where $\mu = 0..3$ denotes a four-vector components). The leading one-body contribution, j^1_μ, represents the photon's interaction with a single nucleon. The many-body contributions are known as meson exchange currents (MEC) and arise from the meson-exchange picture of the nucleon-nucleon (NN) interaction. In that picture, the photon can couple also to mesons exchanged between two nucleons, leading to two-body contributions to the nuclear current. The necessity of introducing the MEC arises from the continuity equation. The momentum and isospin-dependent terms in the potential require the introduction of two-body MEC. Similarly, the inclusion of the three-body force into the Hamiltonian requires the existence of three-body contributions to the nuclear current. However, the effects of the three-body MEC are likely negligible in the low-energy region. Therefore, in the thesis, I will consider one- and two-body currents, only. The continuity equation, connecting the interaction and the current clearly shows that those two quantities should be derived consistently from the same underlying theory of nuclear phenomena. I work with the SMS chiral interaction and for that force the complete consistent MEC has not

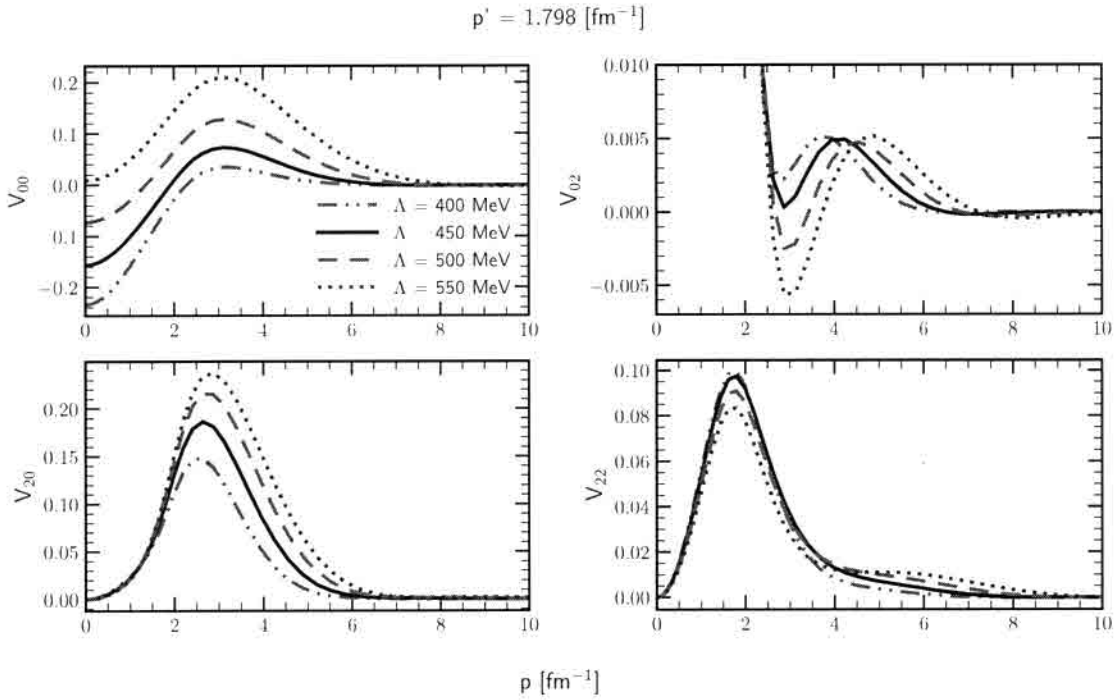

Figure 1.2: Matrix elements $\langle p|V|p'\rangle$ of the SMS potential in coupled partial waves ${}^3S_1 - {}^3D_1$ as a function on the momentum p with fixed value of the momentum $p' = 1.798\,\mathrm{fm}^{-1}$. Potential element $V_{ll'}$ is taken between two states with angular momenta l and l' where $l = 0$ stands for ${}^3S_1$ state and $l = 2$ for ${}^3D_1$.

been derived yet. Consistency includes here also the same regularization as used for the interaction. While the derivation of such currents is ongoing [15], at the moment only SNC is well established. Thus to mimic the effects of the MEC, I apply the Siegert theorem [16, 17]. In general, this theorem allows the substitution of explicit MEC terms by the time component of the nuclear current (the charge density). It is less sensitive to MEC contributions (compared to spatial components of j_μ) and thus in its case, the SNC approximation is sufficient. I use here the formulation of the Siegert theorem given in [17].

A more detailed discussion of electromagnetic currents used here is given in the Sections 2.6. and 2.7, respectively.

and pion absorption operators

CHAPTER 2

FORMALISM AND NUMERICAL METHODS

Even though the deuteron problem was solved a long time ago, I will describe it briefly to introduce the notation and formalism. With that, for more complex 3N cases only a slight extension will be needed.

To calculate any observable for the deuteron photodisintegration, one has to find a nuclear matrix elements:

$$N^{\mu} = \langle \Psi_{final} \mid J^{\mu} \mid \Psi_{initial} \rangle, \tag{2.1}$$

with the two-nucleon wave function of the initial state $\Psi_{initial} = \Psi_{deuteron}$; the two-nucleon wave function of the final scattering state Ψ_{final} and a four-vector current operator J^{μ} which acts between initial and final two-nucleon states. In case of ^{3}He or ^{3}H photodisintegration analogous nuclear matrix element $\langle \Psi_{final} \mid J^{\mu} \mid \Psi_{initial} \rangle$ has to be found, but now $|\Psi_{initial}\rangle$ is either ^{3}He or ^{3}H bound state and $\langle \Psi_{final}|$ describes a 3N scattering state with all three nucleons unbound after reaction or Nd scattering state with the ~~pair nucleon-deuteron~~ in the final state. In the following, I describe how to get these quantities.

2.1 2N bound state

Let's find a deuteron bound state wave function $|\phi_d\rangle$. The time-independent Schrödinger equation for two particles is expressed as:

$$(H_0 + V)\,|\phi_d\rangle = E_d\,|\phi_d\rangle\,, \tag{2.2}$$

with a kinetic energy H_0 and potential V. The kinetic energy H_0 can be represented in terms of relative and total momenta of the particles:

$$H_0 = \frac{\vec{p}_1^{\,2}}{2m_1} + \frac{\vec{p}_2^{\,2}}{2m_2} = \frac{\vec{p}^{\,2}}{2\mu} + \frac{\vec{\mathcal{P}}^2}{2M}, \tag{2.3}$$

where the relative and total momenta are defined as follows:

$$\frac{\vec{p}^2}{2\mu}\phi_l(p) + \sum_{l'=0,2} \int dp' p'^2 \langle p(l1)1m_d| \langle 00|V|00\rangle |p'(l'1)1m_d\rangle \phi_{l'}(p') = E_d \phi_l(p), \quad (2.21)$$

for $l = 0, 2$. In case one does not have a matrix elements for the potential $\langle plm_l \mid V \mid p'l'm'_l\rangle$ in analytical form, but only numerical values for some grid of points are given, there is still one complication in the Eq.(2.21) - integration, which has to be discretized. In order to get rid of the integral I use a Gaussian quadrature method of numerical integration [18]. It allows me to replace an integral by the weighted sum: $\int_a^b f(x)dx = \sum_{i=1}^{N} \omega_i f(x_i)$. In current work I used $N = 72$ points in the interval from 0 to 50 fm^{-1}. Using this method, Eq.(2.21) becomes

$$\frac{p_i^2}{2\mu}\phi_l(p_i) + \sum_{l'=0,2} \sum_{j=0}^{N} \omega_j p_j^2 \langle p_i(l1)1m_d| \langle 00|V|00\rangle |p_j(l'1)1m_d\rangle \phi_{l'}(p_j) = E_d \phi_l(p_i). \quad (2.22)$$

In practical computations, the same grid points p_i are used for p and p' in order to optimize computational time. I solve this equation as an eigenvalue problem $M\Psi = E_d\Psi$ and in that way find simultaneously wave function values in a grid of p points and the binding energy E_d. For example, the binding energy E_d calculated with the SMS potential at different chiral orders is presented in Fig. 2.1.

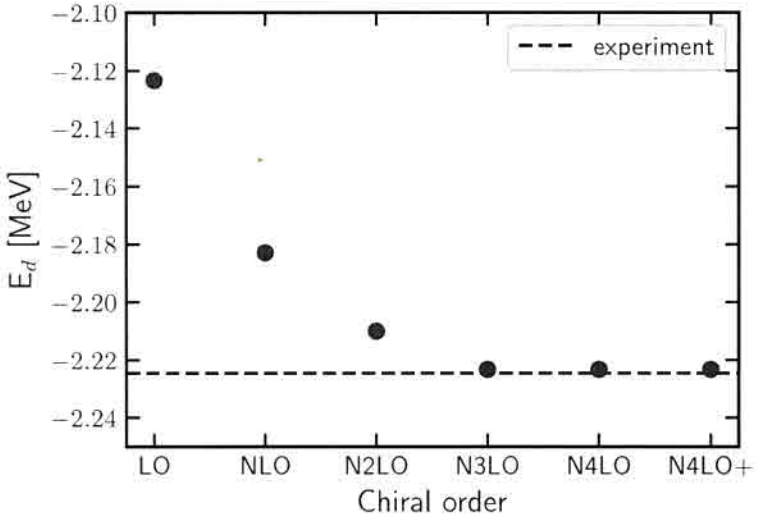

Figure 2.1: Deuteron binding energy calculated using the chiral SMS potential at different chiral orders as a mean value over all cutoffs. Experimental data is taken from [21].

An example of such wave functions is demonstrated in Fig. 2.2. The left panel demonstrates a wave function for $l = 0$ ($^3S_1$) while the right one for $l = 2$ ($^3D_1$). Both plots consist of the curves for different cutoff values and using the chiral SMS potential at N^{4}LO$^+$. The small deviation between lines shows that cutoff dependence is rather weak at this stage but further discrepancies connected to the value of Λ may appear in other components of nuclear matrix elements.

of two nucleons with spin projections m_d and m_n as $\langle \phi m_d m_n|$, we can write Eq. (2.1) as

$$N^\mu = \langle \phi m_d m_n| \left(1 + G_0(E + i\epsilon)t\right) J^\mu \mid \Psi_{deuteron}\rangle \tag{2.34}$$

2.3 3N bound state

The 3N bound state is described by the Schrödinger equation for 3N system, with Hamiltonian comprising two- and three- nucleon interaction. The bound state total wave function $|\Psi\rangle$ obeys the following equation:

$$|\Psi\rangle = G_0(E + i\epsilon) \sum_{j=1}^{3} (V_j + V_4^j) |\Psi\rangle , \tag{2.35}$$

where G_0 is a 3N free propagator as in Eq. (2.27), V_j - is a two-body potential acting between nucleons k and l (j, k and l - numerate nucleons, $j, k, l \in \{1, 2, 3\}$ and $j \neq k \neq l$), V_4^j is a component of three-body potential $V_4 = \sum_{j=1}^{3} V_4^j$ symmetrical under exchange of nucleons k and l, and E - is a 3N binding energy.

Eq. (2.35) can be split into three independent equations for so-called Faddeev components $|\psi_j\rangle$

$$|\Psi\rangle = \sum_{j=1}^{3} |\psi_j\rangle , \tag{2.36}$$

which fulfills separately

$$|\psi_j\rangle = G_0(E + i\epsilon)(V_j + V_4^j) |\Psi\rangle . \tag{2.37}$$

Next, I introduce a permutation operator P, which is a combination of operators P_{jk}:

$$P = P_{12}P_{23} + P_{13}P_{32}. \tag{2.38}$$

The operator P_{jk} acting on the state interchange the momenta and quantum numbers of the nucleons j and k.

Using definitions (2.38) and (2.36), one can rewrite Eq. (2.37) as:

$$|\psi_j\rangle = G_0(E + i\epsilon)t_j P |\psi_j\rangle + (1 + G_0(E + i\epsilon)t_j)G_0(E + i\epsilon)V_4^j(1 + P) |\psi_j\rangle , \tag{2.39}$$

where t_j is a two-body t-operator which obeys Eq. (2.30) for corresponding two-body potential V_j. I solve Eq. (2.39) numerically to find $|\psi_j\rangle$ and the binding energy E. To do that, I perform PWD again.

The partial wave representation of the Eq. (2.39) is obtained using following 3N states:

$$|p, q, \alpha_{J,M_J}\rangle = \left| p, q, (ls)j, (\lambda, \frac{1}{2})I(jI)JM; (t\frac{1}{2})TM_T \right\rangle_1 , \tag{2.40}$$

where index 1 states the choice of the Jacobi momenta, such that p is a relative momentum of the nucleons 2 and 3. Values l, s, and j are quantum numbers in the two-body subsystem consisting of nucleons 2 and 3. λ is the orbital angular momentum with respect to the c.m. of the particles 2 and 3, of the first particle which spin is $\frac{1}{2}$ and I is its total

angular momentum. J and M_J are the total angular momentum of the 3N system and its projection on the z-axis respectively. t is a total isospin of the 2-3 subsystem whereas T and M_T are the total isospin of the 3N system and its projection on the z-axis, respectively. The Jacobi momenta $\vec{p}$ and $\vec{q}$ for three particles with individual momenta $\vec{k}_i, i = 1, 2, 3$ are defined as [19]:

$$\begin{aligned} \vec{p}_i &= \frac{1}{2}(\vec{k}_j - \vec{k}_k), \\ \vec{q}_i &= \frac{1}{3}(2\vec{k}_i - \vec{k}_j - \vec{k}_k), \quad \{i,j,k\} = \{1,2,3\},\{2,3,1\},\{3,1,2\}. \end{aligned} \tag{2.41}$$

2.4 3N scattering state

Let us introduce an asymptotic state $\left|\Phi_j^{3N}\right\rangle$ describing a free motion of three nucleons j,k,l with particles k and l having relative momentum $\vec{p}$ and particle j moving with momentum $\vec{q}$ with respect to the center of mass $(k-l)$ subsystem:

$$\left|\Phi_j^{3N}\right\rangle \equiv \frac{1}{\sqrt{2}}(1 - P_{kl}) \left|\vec{p}(kl)\vec{q}(j)\right\rangle . \tag{2.42}$$

The Jacobi momenta $\vec{p}$ and $\vec{q}$ build the total energy of three nucleons in the 3N-c.m. system:

$$E_{3N} = \frac{|\vec{p}|^2}{m} + \frac{3|\vec{q}|^2}{4m}. \tag{2.43}$$

Using a free propagator $G(E_{3N} - i\epsilon)$ we can come up with the total 3N scattering state

$$\left|\Psi^{(-)}\right\rangle^{3N} = \frac{1}{\sqrt{3}} \sum_j \left|\Psi_j^{(-)}\right\rangle^{3N}, \tag{2.44}$$

where auxiliary scattering states $\left|\Psi_j^{(-)}\right\rangle^{3N}$ are defined as [19]

$$\left|\Psi_j^{(-)}\right\rangle^{3N} \equiv \lim_{\epsilon \to 0} i\epsilon G(E_{3N} - i\epsilon) \left|\Phi_j^{3N}\right\rangle . \tag{2.45}$$

The state $\left|\Psi_j^{(-)}\right\rangle^{3N}$ together with the state $\left|\Phi_j^{3N}\right\rangle$ fulfills an equation [19]

$$\left|\Psi_j^{(-)}\right\rangle^{3N} = \left|\Phi_j^{3N}\right\rangle + G_0 \left(V_1 + V_2 + V_3 + V_4\right) \left|\Psi_j^{(-)}\right\rangle^{3N}. \tag{2.46}$$

Defining the antysymmetrised Faddeev components, and using index "i" instead of "j"

$$\left|F_i^0\right\rangle \equiv G_0 \left(V_i + V_4^i\right) (1 + P) \left|\Psi_i^{(-)}\right\rangle^{3N} \tag{2.47}$$

we obtain a 3N scattering wave function as:

$$\left|\Psi^{(-)}\right\rangle^{Nd} = \frac{1}{\sqrt{3}}(1+P)\left|F_1\right\rangle, \tag{2.55}$$

where

$$\left|F_1\right\rangle = \left|\phi_1^{Nd}\right\rangle G_0(V_1+V_2+V_3+V_4)\sum_{j=1}^{3}\left|\Psi_j^{(-)}\right\rangle^{Nd}. \tag{2.56}$$

The nuclear matrix element $N_\mu^{Nd} = {}^{Nd}\langle\Psi^-|j_\mu|\Psi_i\rangle$ (with Ψ_i - bound state) is now [50, 51]:

$$N_\mu^{Nd} = \frac{1}{\sqrt{3}}\left\langle\Phi_1^{Nd}\right|(1+P)j_\mu\left|\Psi_i\right\rangle + \frac{1}{\sqrt{3}}\left\langle\Phi_1^{Nd}\right|P\left|U_\mu\right\rangle \tag{2.57}$$

with U_μ being a solution of Eq. (2.50). Fact that solving once Eq. (2.50) opens opportunity to compute both N_μ^{Nd} and N_μ^{3N} is a great advantage of the presented formulas.

2.6 Nuclear electromagnetic current

The electromagnetic current operator for 2N (3N) system is constructed from the one- and many-body currents:

$$j_\mu = j_\mu^1 + j_\mu^2(+j_\mu^3). \tag{2.58}$$

Here j_μ^n is a contribution from the interaction between a photon and n nucleons (obviously j_μ^3 is present in 3N system only). Each j_μ^n describes the interaction of photon with all relevant permutations of n nucleons, i.e. j_μ^1 is a sum of photon interactions with each of nucleons in the system separately.

In the case of the photodisintegration process, I will use only a single nucleon current (1NC), so I stick to its definition here. In the Hamiltonian framework, the nucleons are constrained to lie on the mass shell. The general current expression for a single nucleon at the spacetime point zero, denoted as $j_\mu^1(0)$, is computed between the initial nucleon momentum $p \equiv \left(p_0 = \sqrt{M_N^2+\vec{p}^2}, \vec{p}\right)$ and the final momentum $p' \equiv \left(p_0' = \sqrt{M_N^2+\vec{p}'^2}, \vec{p}'\right)$ with the latter one constrained by the four-momentum transfer Q from photon to nucleon. This computation yields the following matrix elements:

$$\begin{aligned}\langle\vec{p}'|j_\mu^1(0)|\vec{p}\rangle &= \bar{u}\left(\vec{p}'s'\right)\left(\gamma^\mu F_1 + i\sigma^{\mu\nu}\left(p'-p\right)_\nu F_2\right)u(\vec{p}s) \\ &= \bar{u}\left(\vec{p}'s'\right)\left(G_M\gamma^\mu - F_2\left(p'+p\right)^\mu\right)u(\vec{p}s).\end{aligned} \tag{2.59}$$

In the above equation, the symbols $u(\vec{p}s)$ represent Dirac spinors for particle having momentum $\vec{p}$ and spin s, F_1 and F_2 are the Dirac and Pauli form factors of the nucleon, respectively, and $G_M \equiv F_1 + 2M_N F_2$ denotes the magnetic form factor of the nucleon. The proton charge e is extracted from the matrix element. Further γ^μ are Dirac matrices and $\sigma^{\mu\nu} = \frac{i}{2}[\gamma^\mu, \gamma^\nu]$. In this thesis, only the nonrelativistic limit of Eq. (2.59) is considered, which leads to well-known expressions for the operators for the single nucleon current [53]:

$$\langle \vec{p}' | j_0^1 | \vec{p} \rangle = \left(G_E^p \Pi^p + G_E^n \Pi^n \right), \tag{2.60}$$

$$\langle \vec{p} | j^{\vec{1}} | \vec{p} \rangle = \frac{\vec{p} + \vec{p}'}{2M_N} \left(G_E^p \Pi^p + G_E^n \Pi^n \right) + \frac{i}{2M_N} \left(G_M^p \Pi^p + G_M^n \Pi^n \right) \vec{\sigma} \times (\vec{p}' - \vec{p}) \,. \tag{2.61}$$

The electric form factor denoted as G_E is defined as $G_E \equiv F_1 + \frac{(p'-p)^2}{2M_N} F_2$ and represents the neutron (n) and proton (p) form factors. Both electric and magnetic form factors, $G_E \equiv G_E(Q^2)$, and $G_M(Q^2)$, are normalized as:

$$\begin{aligned} G_E^n(0) &= 0 \\ G_E^p(0) &= 1 \\ G_M^n(0) &= -1.913 \\ G_M^p(0) &= 2.793 \end{aligned} \tag{2.62}$$

The above values correspond to nucleons with point-like characteristics. While all the form factors depend on the squared four-momentum transfer $(p' - p)^2$, in the nonrelativistic regime, it is common to use as arguments of G_E and G_M the squared three-momentum transfer $-(\vec{p}' - \vec{p})^2$ or even set it to zero for interactions involving real photons. Numerous authors have investigated the properties of electromagnetic nucleon form factors through theoretical and experimental approaches, as discussed in [54, 55] but at low energies discussed here, all models lead to practically the same values of the form factors. Π^p (Π^n) in Eq. (2.61) is a proton (neutron) isospin projection operator.

The two-nucleon current contribution is in that work taken into account via Siegert approach [16, 17, 53]. To do that we break down the single nucleon current matrix elements into multipole components and represent some of the electric multipoles using the Coulomb multipoles, which arise from the single nucleon charge density operator [53]. This is acceptable because, in low-energy regime, contributions from many nucleons to the nuclear charge density are typically small. We then obtain the rest of the electric multipoles and all of the magnetic multipoles exclusively from the single nucleon current operators.

In 3N system we have following expressions for the 1NC:

$$\langle \vec{p}', \vec{q}' | j_0^1 | \vec{p}, \vec{q} \rangle = \int d\vec{p}'' d\vec{q}'' \left\langle \vec{p}', \vec{q}' \middle| \frac{1}{2}\left(1+\tau(1)_z\right) F_1^p + \frac{1}{2}\left(1-\tau(1)_z\right) F_1^n \middle| \vec{p}'', \vec{q}'' \right\rangle \left\langle \vec{p}'', \vec{q}'' - \frac{2}{3}\vec{Q} \middle| \vec{p}, \vec{q} \right\rangle \tag{2.63}$$

$$\langle \vec{p}', \vec{q}' | j_\pm^{1,\,\mathrm{conv}} | \vec{p}, \vec{q} \rangle = \frac{1}{m} \int d\vec{p}'' d\vec{q}'' \langle \vec{p}', \vec{q}' | \left[\frac{1}{2}\left(1+\tau(1)_z\right) F_1^p + \frac{1}{2}\left(1-\tau(1)_z\right) F_1^n \right] q_\pm | \vec{p}'', \vec{q}'' \rangle \left\langle \vec{p}'', \vec{q}'' - \frac{2}{3}\vec{Q} \middle| \vec{p}, \vec{q} \right\rangle \tag{2.64}$$

$$\langle \vec{p}', \vec{q}' | j_\pm^{1,spin} | \vec{p}, \vec{q} \rangle = \frac{i}{2m} \int d\vec{p}'' d\vec{q}'' \langle \vec{p}', \vec{q}' | * \left[\frac{1}{2}\left(1+\tau(1)_z\right)\left(F_1^p + 2mF_2^p\right) + \frac{1}{2}\left(1-\tau(1)_z\right)\left(F_1^n + 2mF_2^n\right) \right] * \left(\vec{\sigma}(1) \times \vec{Q}\right)_\pm | \vec{p}'', \vec{q}'' \rangle \left\langle \vec{p}'', \vec{q}'' - \frac{2}{3}\vec{Q} \middle| \vec{p}, \vec{q} \right\rangle . \tag{2.65}$$

In Eq. (2.64) and Eq. (2.65) we present convection and spin currents which combined together form a spatial component of the single nucleon current $\vec{j}^1(\mu) \equiv \vec{j}^1(\mu, conv) + \vec{j}^1(\mu, spin)$. In my thesis I use a ~~model of~~ M. Garu and W. Krümpelmann [56] for which:

$$F_1^p(0) = 1 \qquad 2mF_2^p(0) = 1.793 \tag{2.66}$$

$$F_1^n(0) = 0 \qquad 2mF_2^n(0) = -1.913 \tag{2.67}$$

2.7 Pion absorption

For the pion absorption, I include explicitly two nucleon current (2NC) as well as 1NC. Thus the absorption operator is $\rho = \rho(1) + \rho(1,2)$, where absorption on a single nucleon is included in $\rho(1)$ and $\rho(1,2)$ plays a role of two-body ~~charge current~~. The matrix element of the single nucleon pion absorption operator $\rho(1)$ in momentum-space for nucleon 1 relies on the nucleon's incoming momentum ($\vec{p}$) and outgoing momentum ($\vec{p}'$) [57]:

$$\langle \vec{p}' | \rho(1) | \vec{p} \rangle = -\frac{g_A M_\pi}{\sqrt{2} F_\pi} \frac{(\vec{p}' + \vec{p}) \cdot \vec{\sigma}_1}{2M} (\vec{\tau}_1)_- , \tag{2.68}$$

where the values of the nucleon axial vector coupling, pion decay constant, and negative pion mass are $g_A = 1.29$, $F_\pi = 92.4\,\mathrm{MeV}$, and $M_\pi = 139.57\,\frac{\mathrm{MeV}}{c^2}$, respectively. $\rho(1)$ operates in the spin and isospin spaces and involves the Pauli spin (isospin) operator $\vec{\sigma}_1$ ($\vec{\tau}_1$) for nucleon 1 and the isospin lowering operator $(\vec{\tau}_1)_- \equiv ((\vec{\tau}_1)_x - \mathrm{i}(\vec{\tau}_1)_y)/2$. As before I use the average "nucleon mass" $M \equiv \frac{1}{2}(M_p + M_n,)$ where the proton mass is M_p and neutron mass is M_n.

The 2N part of ρ at LO has the form [58]

$$\langle \vec{p}_1', \vec{p}_2' | \rho(1,2) | \vec{p}_1\, \vec{p}_2 \rangle = \left(v(k_2)\vec{k}_2 \cdot \vec{\sigma}_2 - v(k_1)\vec{k}_1 \cdot \vec{\sigma}_1 \right) \times \frac{i}{\sqrt{2}} \left[\left(\vec{\tau}_1 \times \vec{\tau}_2\right)_x - i\left(\vec{\tau}_1 \times \vec{\tau}_2\right)_y \right] , \tag{2.69}$$

where $\vec{k}_1 = \vec{p}_1' - \vec{p}_1$, $\vec{k}_2 = \vec{p}_2' - \vec{p}_2$ and the formfactor $v(k)$ reads

$$v(k) = \frac{1}{(2\pi)^3} \frac{g_A M_\pi}{4F_\pi^3} \frac{1}{M_\pi^2 + k^2} . \tag{2.70}$$

In the case of the pion absorption process, we follow a standard procedure including partial wave states for both 2N and 3N induced nuclei. It occurs that in such a case one needs current matrix elements. For 2N this is $\left\langle \vec{p} + \frac{1}{2}\vec{P}_f \middle| \rho(1) \middle| \vec{p} - \frac{1}{2}\vec{P}_f + \vec{P}_i \right\rangle$ and for 3N case $\left\langle \vec{q} + \frac{1}{3}\vec{P}_f \middle| \rho(1) \middle| \vec{q} - \frac{2}{3}\vec{P}_f + \vec{P}_i \right\rangle$.

For the $\pi^- + {}^2\mathrm{H} \to n + n$ reaction, the nuclear matrix element for the transition operator is given by:

$$N_{nn}(m_1, m_2, m_d) \;=\; {}^{(-)}\left\langle \vec{p}_0\, m_1\, m_2\;\vec{P}_f = 0 \middle| \rho \middle| \phi_d\, m_d\;\vec{P}_i = 0 \right\rangle , \tag{2.71}$$

where $\left| \vec{p}_0\, m_1\, m_2\;\vec{P}_f = 0 \right\rangle^{(-)}$ denotes the 2N scattering state [70]. The total absorption rate for this reaction expresses as:

$$\Gamma_{nn} = \frac{(\alpha\, M_d')^3\; c\, M_n\, p_0}{2M_{\pi^-}} \int d\hat{p}_0\, \frac{1}{3} \sum_{m_1, m_2, m_d} |N_{nn}(m_1, m_2, m_d)|^2 . \tag{2.72}$$

Turning to 3N system I investigate pion absorption in ^{3}He or ^{3}H with various final states. For $\pi^- + {}^3\mathrm{He} \to n + d$ reaction the most important step in obtaining predictions is calculating the matrix element of the 3N transition operator ρ_{3N}, which is the ρ acting between the initial ^{3}He and the final Nd scattering state immersed in 3N space:

$$N_{nd}(m_n, m_d, m_{^3\mathrm{He}}) \equiv {}^{(-)}\left\langle \Psi_{nd}\, m_n\, m_d\, \vec{P}_f = 0 \middle| \rho_{3N} \middle| \Psi_{^3\mathrm{He}}\, m_{^3\mathrm{He}}\, \vec{P}_i = 0 \right\rangle . \tag{2.73}$$

Given Eq. (2.73) the total absorption rate may be obtained from the following:

$$\Gamma_{nd} = \mathcal{R}\, \frac{16\, \left(\alpha^3\, M_{^3\mathrm{He}}'\right)^3\; c\, M q_0}{9 M_{\pi^-}} \int d\hat{q}_0\, \frac{1}{2} \sum_{m_n, m_d, m_{^3\mathrm{He}}} |N_{nd}(m_n, m_d, m_{^3\mathrm{He}})|^2 , \tag{2.74}$$

where $M_{^3\mathrm{He}}' = \frac{M_{^3\mathrm{He}} M_{\pi^-}}{M_{^3\mathrm{He}} + M_{\pi^-}}$ is now the reduced mass of the $\pi^- - {}^3\mathrm{He}$ system. The factor $\mathcal{R} = 0.98$ appears due to the finite volume of the ^{3}He charge [70]. The final state energy is expressed in terms of the neutron momentum $\vec{q}_0$

$$M_\pi + M_{^3\mathrm{He}} \approx M_n + M_d + \frac{3}{4}\frac{\vec{q}_0^{\,2}}{M} , \tag{2.75}$$

The full 3N breakup is calculated in a similar way and the total absorption rate for $\pi^- + {}^3\mathrm{He} \to p + n + n$ reaction is defined as follows

$$\Gamma_{pnn} = \mathcal{R}\,\frac{16\,\left(\alpha\,M'_{^3\mathrm{He}}\right)^3\,c\,M}{9M_{\pi^-}}\int d\hat{q}\int_0^{2\pi} d\phi_p \int_0^{\pi} d\theta_p \sin\theta_p$$
$$\times \int_0^{p_{max}} dpp^2\,\sqrt{\frac{4}{3}\left(M E_{pq} - p^2\right)}\,\frac{1}{2}\sum_{m_1,m_2,m_3,m_{^3\mathrm{He}}} |N_{pnn}(m_1,m_2,m_3,m_{^3\mathrm{He}})|^2 \qquad (2.76)$$

with

$$N_{pnn}(m_1,m_2,m_3,m_{^3\mathrm{He}}) \equiv {}^{(-)}\left\langle \Psi_{pnn}\,m_1\,m_2\,m_3\,\vec{P}_f=0\right|\rho_{3N}\left|\Psi_{^3\mathrm{He}}\,m_{^3\mathrm{He}}\,\vec{P}_i=0\right\rangle \qquad (2.77)$$

E_{pq} is the internal energy of the final 3N state and can be expressed in terms of the Jacobi relative momenta $\vec{p}$ and $\vec{q}$

$$M_\pi + M_{^3\mathrm{He}} \approx 3M + \frac{\vec{p}^{\,2}}{M} + \frac{3}{4}\frac{\vec{q}^{\,2}}{M} \equiv 3M + E_{pq} = 3M + \frac{p_{max}^2}{M} = 3M + \frac{3}{4}\frac{q_{max}^2}{M}\,. \qquad (2.78)$$

In Eq. (2.78) p_{max} and q_{max} are maximal kinematically allowed values of Jacobi momenta p and q, respectively.

Analogously, the total absorption rate for $\pi^- + {}^3\mathrm{H} \to n+n+n$ reads

$$\Gamma_{nnn} = \frac{2\,\left(\alpha\,M'_{^3\mathrm{H}}\right)^3\,c\,M}{27M_{\pi^-}}\int d\hat{\mathbf{q}}\int_0^{2\pi} d\phi_p \int_0^{\pi} d\theta_p \sin\theta_p$$
$$\times \int_0^{p_{max}} dpp^2\,\sqrt{\frac{4}{3}\left(M E_{pq} - p^2\right)}\,\frac{1}{2}\sum_{m_1,m_2,m_3,m_{^3\mathrm{H}}} |N_{nnn}(m_1,m_2,m_3,m_{^3\mathrm{H}})|^2 \qquad (2.79)$$

with

$$N_{nnn}(m_1,m_2,m_3,m_{^3\mathrm{H}}) \equiv {}^{(-)}\left\langle \Psi_{nnn}\,m_1\,m_2\,m_3\,\vec{P}_f=0\right|\rho_{3N}\left|\Psi_{^3\mathrm{H}}\,m_{^3\mathrm{H}}\,\vec{P}_i=0\right\rangle\,. \qquad (2.80)$$

In the Results section, I also demonstrate (for processes with three free nucleons in the final state) predictions of the differential absorption rates. The natural domain is defined by energies of outgoing nucleons (E_1, E_2); in such a case the differential absorption rate $d^2\Gamma_{pnn}/\left(dE_1\,dE_2\right)$ expresses as [59]

$$\frac{d^2\Gamma_{pnn}}{dE_1\,dE_2} = \mathcal{R}\,\frac{64\,\pi^2\,\left(\alpha\,M'_{^3\mathrm{He}}\right)^3\,c\,M^3}{3M_{\pi^-}}$$
$$\times\frac{1}{2}\sum_{m_1,m_2,m_3,m_{^3\mathrm{He}}} |N_{pnn}(m_1,m_2,m_3,m_{^3\mathrm{He}})|^2\,. \qquad (2.81)$$

The kinematically allowed region is restricted to energies fulfilling the condition

If we define the difference between observables at each subsequent order as:

$$\Delta X^{(2)} = |X^{(2)} - X^{(0)}|, \qquad \Delta X^{(i>2)} = |X^{(i)} - X^{(i-1)}|, \tag{2.84}$$

than chiral expansion for X can be written as:

$$X = X^{(0)} + \Delta X^{(2)} + \Delta X^{(3)} + ... + \Delta X^{(i)}. \tag{2.85}$$

The truncation error at i-th order, $\delta X^{(i)}$, is estimated using values of the observable obtained at lower orders as follows:

$$\delta X^{(0)} = Q^2 \left| X^{(0)} \right|, \tag{2.86}$$

$$\delta X^{(i)} = \max_{2 \le j \le i} \left(Q^{i+1} \left| X^{(0)} \right|, Q^{i+1-j} \left| \Delta X^{(j)} \right| \right). \tag{2.87}$$

Additionally, following [63] I use the actual high-order predictions (if known) to specify uncertainties at lower orders, so that:

$$\delta X^{(i)} \geq \max_{j,k} (|X^{j \geq i} - X^{k \geq i}|) \tag{2.88}$$

and to be conservative I use additional restriction:

$$\delta X^{(i)} \geq Q \delta X^{(i-1)}. \tag{2.89}$$

All the conditions above assume that we use the whole available information at hand. In [66] it was shown that such a method is equivalent to the Bayesian approach proposed there.

Cut-off dependence

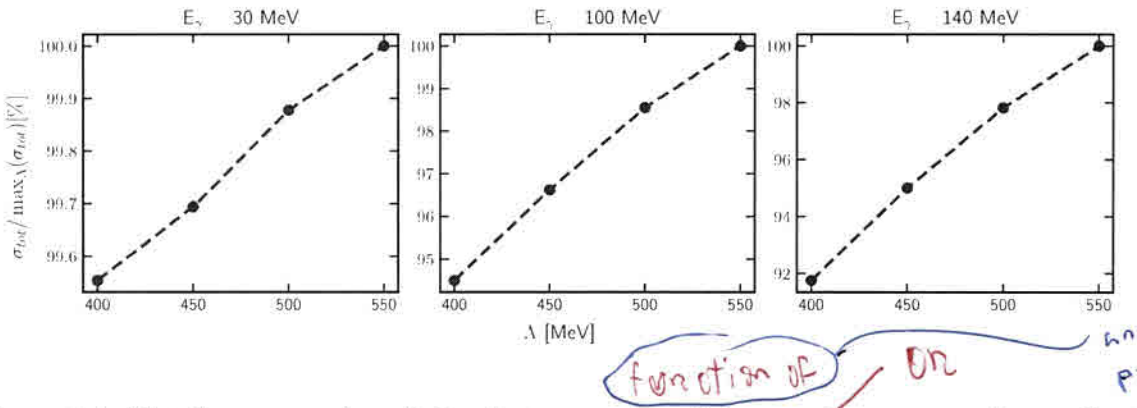

Figure 2.3: Total cross section of the deuteron photodisintegration process (normalized to the maximal cross section among all Λ) as a dependence of the cutoff parameter Λ for three photon energy E_γ values: 30, 100, and 140 MeV.

Another theoretical uncertainty comes from the choice of the cutoff parameter's value of regulator described in the Chapter 1.